Electronic Supplementary Information (ESI)

for *NJC*

Synthesis, crystal structure and magnetic properties of octanuclear Ni₄Ln₄ complexes constructed by Schiff base ligand and di-2-pyridyl ketone†

Yu-Jie Zhu,[a] Hui-Sheng Wang,[*a] Yuxiang Chen,[*b] Pengfei Zhou,[a] Yanfang Wu[c] and Yi-Quan Zhang[*d]

[a.] School of Chemistry and Environmental Engineering, Key Laboratory of Green Chemical Process of Ministry of Education, Hubei Key Laboratory of Novel Reactor and Green Chemical Technology, Wuhan Institute of Technology, Wuhan 430074, P. R. China.

[b.] School of Pharmaceutical and Chemical Engineering, Taizhou University, Taizhou 318000, P.R. China.

[c.] School of Energy and Mechanical Engineering, Jiangxi University of Science and Technology, Nanchang 330013, P. R. China.

[d.] Jiangsu Key Laboratory for NSLSCS, School of Physical Science and Technology, Nanjing Normal University, Nanjing 210023, P.R. China

*E-mail: wangch198201@163.com (H. S. Wang), cyx@tzc.edu.cn (Y. Chen), zhangyiquan@njnu.edu.cn (Y.Q. Zhang).

Table S1. Crystallographic data for complexes **1-3**

Complexes	1	2	3
Formula[a]	$C_{126}H_{166}Dy_4N_{20}Ni_4O_{55}$	$C_{126}H_{164}Dy_{0.09}N_{20}Ni_4O_{54}Y_{3.91}$	$C_{126}H_{162}N_{20}Ni_4O_{53}Y_4$
Formula weight[a]	3725.54	3419.77	3395.13
Crystal color	yellow	yellow	yellow
Crystal size (mm)^3	$0.13 \times 0.10 \times 0.07$	$0.26 \times 0.23 \times 0.19$	$0.27 \times 0.24 \times 0.21$
Crystal system	monoclinic	monoclinic	monoclinic
Space group	$C2/c$	$C2/c$	$C2/c$
a (Å)	48.1535(19)	48.0558(15)	48.1240(17)
b (Å)	19.3949(8)	19.4125(6)	19.4411(7)
c (Å))	15.7658(5)	15.7368(4)	15.7458(7)
α (°)	90	90	90
β (°)	99.221(2)	99.2650(10)	99.3450(10)
γ (°)	90	90	90
Unit cell volume (Å^3)	14533.9(10)	14489.1(7)	14536.0(10)
T (K)	173(2)	172(2)	173(2)
Z	4	4	4
Radiation type	Mo/$K\alpha$	Mo/$K\alpha$	Mo/$K\alpha$
Wavelength (Å)	0.71073	0.71073	0.71073
μ (mm^{-1})	2.607	2.173	2.155
D_c (g cm^{-3})	1.449	1.322	1.314
θ range	$2.71 \sim 25.34$	$2.62 \sim 25.31$	$2.62 \sim 25.35$
Index ranges	$-57 \le h \le 55$	$-57 \le h \le 57$	$-57 \le h \le 57$
	$-23 \le k \le 23$	$-21 \le k \le 23$	$-23 \le k \le 23$
	$-18 \le l \le 17$	$-18 \le l \le 18$	$-18 \le l \le 18$
$F(000)$	6272	5850	5840
Reflections collected	34331	53553	41532
Unique reflections [R_{int}]	12663 [0.0755]	12702	12758 [0.0706]
Reflections with $I > 2\sigma(I)$	7866	8842	8659
Restraints/parameters	0/799	0/805	0/798
Final R indexes [$I >= 2\sigma$ (I)][b,c]	$R_1 = 0.0616$, $wR_2 = 0.1525$	$R_1 = 0.0565$, $wR_2 = 0.1628$	$R_1 = 0.0594$, $wR_2 = 0.1775$
Final R indexes [all data]	$R_1 = 0.1201$, $wR_2 = 0.1698$	$R_1 = 0.0989$, $wR_2 = 0.1832$	$R_1 = 0.1010$, $wR_2 = 0.1976$
S (all data)	1.099	1.099	1.098
$(\Delta\rho)_{max,min}$/e Å^{-3}	2.934 and -2.694	1.932 and -0.734	1.947 and -0.801

[a] The formula and the formula weights include the solvent molecules which were subtracted by SQUEEZE program.

[b] $R_1 = \Sigma (||F_o| - |F_c||)/\Sigma|F_o|$. [c] $wR_2 = [\Sigma [w (F_o^2 - F_c^2)^2]/\Sigma [w (F_o^2)^2]]^{0.5}$, w = $1/[\sigma^2(F_o^2) + [(ap)^2 + bp]$, where $p = [max(F_o^2, 0) + 2F_c^2]/3$.

Table S2. Selected bond lengths (Å) and angles (°) for **1**.

Selected bond lengths for **1**					
Dy1-O2	2.184(6)	Dy2-O10	2.382(5)	Ni1-O4^i	2.080(6)
Dy1-O5	2.265(6)	Dy2-O14	2.380(6)	Ni1-O1	2.074(5)
Dy1-O14	2.342(5)	Dy2-O15	2.376(7)	Ni1-O1^i	2.111(5)
Dy1-O10	2.391(6)	Dy2-O16	2.378(8)	Ni2-O7	2.058(7)
Dy1-O4	2.446(5)	Dy2-N10	2.506(8)	Ni2-O8	2.053(6)
Dy1-O1	2.459(5)	Dy2-O9	2.529(6)	Ni2-O11	2.059(7)
Dy1-N2	2.480(6)	Ni1-N4^i	2.012(6)	Ni2-N6	2.029(8)
Dy1-O6	2.542(5)	Ni1-O13	2.040(6)	Ni2-N8	2.154(8)
Dy2-O11	2.293(7)	Ni1-O5	2.034(6)	Ni2-N9	2.073(8)
Dy2-O8	2.283(7)				

Selected bond angles for **1**					
O2-Dy1-O5	148.34(19)	O11-Dy2-O14	104.5(2)	O5-Ni1-O4^i	168.4(2)
O2-Dy1-O14	121.5(2)	O8-Dy2-O14	145.9(2)	N4^i-Ni1-O1	172.0(3)
O5-Dy1-O14	80.6(2)	O10-Dy2-O14	66.01(18)	O13-Ni1-O1	90.7(2)
O2-Dy1-O10	79.4(2)	O14-Dy2-O15	55.2(2)	O5-Ni1-O1	83.4(2)
O5-Dy1-O10	91.4(2)	O11-Dy2-O16	99.1(3)	O4^i-Ni1-O1	105.6(2)
O14-Dy1-O10	66.46(19)	O8-Dy2-O16	80.4(2)	N4^i-Ni1-O1^i	98.9(2)
O2-Dy1-O4	86.3(2)	O10-Dy2-O16	155.3(2)	O13-Ni1-O1^i	170.8(2)
O5-Dy1-O4	88.18(18)	O14-Dy2-O16	132.7(2)	O1-Ni1-O1^i	81.2(2)
O10-Dy1-O1	135.88(18)	O15-Dy2-O16	82.6(3)	N6-Ni2-O7	83.1(3)
O5-Dy1-N2	136.3(2)	O11-Dy2-N10	67.6(3)	O11-Ni2-N8	88.0(3)
O14-Dy1-N2	81.6(2)	O8-Dy2-N10	126.6(3)	N6-Ni2-O8	87.4(3)
O10-Dy1-N2	117.0(2)	O10-Dy2-N10	131.3(3)	O7-Ni2-O8	170.3(3)
O4-Dy1-N2	81.2(2)	O14-Dy2-N10	78.9(3)	N6-Ni2-O11	168.9(3)
O5-Dy1-O6	63.63(18)	O11-Dy2-O9	136.7(2)	O7-Ni2-O11	107.7(3)
O14-Dy1-O6	126.76(18)	O8-Dy2-O9	64.7(2)	O8-Ni2-O11	81.9(3)
O4-Dy1-O6	78.73(17)	N10-Dy2-O9	145.5(3)	N6-Ni2-N9	100.1(3)
O1-Dy1-O6	124.48(19)	N4^i-Ni1-O13	89.8(2)	O8-Ni2-N9	93.3(3)
N2-Dy1-O6	151.0(2)	N4^i-Ni1-O5	88.6(2)	O11-Ni2-N9	77.9(3)
O11-Dy2-O8	72.1(2)	O13-Ni1-O5	93.3(2)	O8-Ni2-N8	92.6(3)
O11-Dy2-O10	88.8(2)	N4^i-Ni1-O4^i	82.3(2)	N9-Ni2-N8	163.7(3)

Symmetry code: ^{i} $0.5 - x$, $0.5 - y$, $1 - z$.

Table S3. Selected bond lengths (Å) and angles (°) for **3**.

Selected bond lengths for 3					
Y1-O2	2.170(4)	Y2-O10	2.349(4)	Ni1-O4^i	2.086(4)
Y1-O5	2.274(4)	Y2-O14	2.373(4)	Ni1-O1	2.066(4)
Y1-O14	2.312(4)	Y2-O15	2.358(4)	Ni1-O1^i	2.110(4)
Y1-O10	2.395(4)	Y2-O16	2.368(4)	Ni2-O7	2.062(5)
Y1-O4	2.416(4)	Y2-N10	2.498(5)	Ni2-O8	2.056(4)
Y1-O1	2.440(4)	Y2-O9	2.510(4)	Ni2-O11	2.066(4)
Y1-N2	2.470(4)	Ni1-N4^i	2.014(5)	Ni2-N6	2.035(5)
Y1-O6	2.540(4)	Ni1-O13	2.051(4)	Ni2-N8	2.151(5)
Y2-O11	2.270(4)	Ni1-O5	2.015(4)	Ni2-N9	2.077(5)
Y2-O8	2.271(4)				

Selected bond angles for 3					
O2-Y1-O5	147.60(14)	O11-Y2-O14	104.17(14)	O5-Ni1-O4^i	167.47(15)
O2-Y1-O14	121.56(14)	O8-Y2-O14	146.08(14)	N4^i-Ni1-O1	171.49(17)
O5-Y1-O14	80.93(13)	O10-Y2-O14	65.84(13)	O13-Ni1-O1	90.29(15)
O2-Y1-O10	78.93(14)	O14-Y2-O15	55.75(14)	O5-Ni1-O1	83.47(15)
O5-Y1-O10	91.89(13)	O11-Y2-O16	98.28(17)	O4^i-Ni1-O1	105.87(14)
O14-Y1-O10	66.06(13)	O8-Y2-O16	80.12(15)	N4^i-Ni1-O1^i	98.50(16)
O2-Y1-O4	86.17(14)	O10-Y2-O16	156.09(14)	O13-Ni1-O1^i	170.38(14)
O5-Y1-O4	88.15(13)	O14-Y2-O16	132.96(15)	O1-Ni1-O1^i	81.20(15)
O10-Y1-O1	135.69(13)	O15-Y2-O16	82.59(16)	N6-Ni2-O7	82.7(2)
O5-Y1-N2	136.72(14)	O11-Y2-N10	67.14(16)	O11-Ni2-N8	87.94(18)
O14-Y1-N2	81.31(15)	O8-Y2-N10	126.73(15)	N6-Ni2-O8	88.05(19)
O10-Y1-N2	115.91(14)	O10-Y2-N10	130.07(16)	O7-Ni2-O8	170.50(17)
O4-Y1-N2	81.61(13)	O14-Y2-N10	78.28(15)	N6-Ni2-O11	169.0(2)
O5-Y1-O6	64.16(13)	O11-Y2-O9	137.28(14)	O7-Ni2-O11	108.16(17)
O14-Y1-O6	127.05(13)	O8-Y2-O9	65.12(14)	O8-Ni2-O11	81.09(16)
O4-Y1-O6	78.74(12)	N10-Y2-O9	145.76(17)	N6-Ni2-N9	101.3(2)
O1-Y1-O6	124.77(12)	N4^i-Ni1-O13	90.59(17)	O8-Ni2-N9	93.31(19)
N2-Y1-O6	150.72(15)	N4^i-Ni1-O5	88.03(17)	O11-Ni2-N9	77.97(18)
O11-Y2-O8	72.33(14)	O13-Ni1-O5	93.42(15)	O8-Ni2-N8	92.35(18)
O11-Y2-O10	88.63(15)	N4^i-Ni1-O4^i	82.49(16)	N9-Ni2-N8	163.8(2)

Symmetry code: ^{i} $0.5 - x$, $0.5 - y$, $1 - z$.

Table S4. Bond valence sum (BVS) calculations for determining of the protonation levels of the O atoms from the ligands in **1** and **3**.

Atoms in **1**	BVS values of **1**	Atoms in **3**	BVS values of **3**
O1	2.04	O1	2.02
O2	2.03	O2	1.91
O3	1.95	O3	1.98
O4	1.87	O4	1.78
O5	2.08	O5	2.05
O6	2.08	O6	2.06
O7	1.54	O7	1.50
O8	2.05	O8	2.02
O9	2.10	O9	2.06
O10	1.88	O10	1.85
O11	1.84	O11	1.82
O12	1.77	O12	1.80
O13	1.89	O13	1.86
O14	2.06	O14	2.01
O15	1.55	O15	1.65
O16	1.18	O16	1.25

Note:

1) The values of BVS calculations for O atoms in the 1.8-2.0, 1.0-1.2, and 0.2-0.4 ranges are indicative of non-, single- and double-protonation, respectively.

2) The O atoms with single-protonation were labeled by red.

3) Although the BVS values of O7 atoms in **1** and **3** are only 1.54 and 1.50, respectively, the two O atoms were assigned as non-protonation according to the charge balance of complexes **1** and **3**.

Table S5. Bond valence sum (BVS) calculations for determining of the oxidation states of the Dy and Ni atoms in **1** as well as the Y and Ni atoms in **3**.

Ni and Dy atoms in **1**		Ni and Y atoms in **3**	
Dy1	3.38	Y1	3.29
Dy2	3.27	Y2	3.24
Ni1	2.13	Ni1	2.14
Ni2	2.23	Ni2	2.21

Table S6. The possible geometries of oct-coordination metal centers and Deviation parameters from each ideal polyhedron for Dy1 and Dy2 in **1**.

Point group	Geometry	Polyhedron	CShM of Dy1	CShM of Dy2
D_{8h}	OP-8	Octagon	31.297	34.298
C_{7v}	HPY-8	Heptagonal pyramid	23.523	22.721
D_{6h}	HBPY-8	Hexagonal bipyramid	14.620	11.735
O_h	CU-8	Cube	10.303	8.851
D_{4d}	SAPR-8	Square antiprism	2.495	2.898
D_{2d}	TDD-8	Triangular dodecahedron	1.859	2.862
D_{2d}	JGBF-8	Johnson - Gyrobifastigium (J26)	12.139	11.024
D_{3h}	JETBPY-8	Johnson - Elongated triangular bipyramid (J14)	28.075	25.472
C_{2v}	JBTPR-8	Johnson - Biaugmented trigonal prism (J50)	1.954	3.687
C_{2v}	BTPR-8	Biaugmented trigonal prism	1.571	3.314
D_{2d}	JSD-8	Snub disphenoid (J84)	4.375	5.706
T_d	TT-8	Triakis tetrahedron	10.994	9.596
D_{3h}	ETBPY-8	Elongated trigonal bipyramid	22.935	19.436

Note: The coordination geometries of Dy1 and Dy2 were labeled by red.

Table S7. The possible geometries of oct-coordination metal centers and Deviation parameters from each ideal polyhedron for Y1 and Y2 in **3**.

Point group	Geometry	Polyhedron	CShM of Dy1	CShM of Dy2
D_{8h}	OP-8	Octagon	32.071	34.315
C_{7v}	HPY-8	Heptagonal pyramid	23.576	22.870
D_{6h}	HBPY-8	Hexagonal bipyramid	14.848	11.659
O_h	CU-8	Cube	10.400	8.751
D_{4d}	SAPR-8	Square antiprism	2.492	2.904
D_{2d}	TDD-8	Triangular dodecahedron	1.783	2.732
D_{2d}	JGBF-8	Johnson - Gyrobifastigium (J26)	12.293	10.968
D_{3h}	JETBPY-8	Johnson - Elongated triangular bipyramid (J14)	27.874	25.699
C_{2v}	JBTPR-8	Johnson - Biaugmented trigonal prism (J50)	1.930	3.591
C_{2v}	BTPR-8	Biaugmented trigonal prism	1.576	3.233
D_{2d}	JSD-8	Snub disphenoid (J84)	4.354	5.638
T_d	TT-8	Triakis tetrahedron	11.139	9.500
D_{3h}	ETBPY-8	Elongated trigonal bipyramid	23.372	19.740

Note: The coordination geometries of Y1 and Y2 were labeled by red.

Table S8. Best fitted parameters obtained from the fits of the Cole-Cole plots of **1** under a zero dc field by employing a double relaxation Debye model.

T (K)	χ_S	χ_{T1}	τ_1 (s)	α_1	χ_{T2}	τ_2 (s)	α_2	Residual
1.90009	0.40984	3.23106	0.02487	0.28848	4.95093	0.00105	0.54468	0.00997
1.99988	0.45978	3.13235	0.01639	0.28029	4.5166	7.71413E-4	0.5163	0.01343
2.10001	0.53369	2.90923	0.01127	0.25272	4.16502	6.05971E-4	0.48122	0.01145
2.20016	0.5801	2.92971	0.0079	0.24804	3.70863	4.38632E-4	0.44734	0.0122
2.29999	0.59123	2.83022	0.00574	0.24175	3.45053	3.44225E-4	0.42597	0.01201
2.40005	0.63135	2.75819	0.00427	0.22917	3.15205	2.70412E-4	0.39448	0.01389
2.50001	0.64819	2.56422	0.00336	0.2155	3.05066	2.3542E-4	0.37841	0.01238
2.60004	0.6106	2.54921	0.00254	0.21153	2.82855	1.75794E-4	0.35535	0.01203
2.79979	0.38188	2.64895	0.00146	0.21701	2.49271	8.15123E-5	0.31911	0.01006
2.99986	1.12696E-5	2.62218	9.37412E-4	0.20676	2.47789	3.97407E-5	0.23927	0.0088
3.20007	2.92976E-5	2.5045	6.54413E-4	0.1941	2.22683	3.40941E-5	0.08868	0.00611
3.40008	7.60069E-5	2.26478	5.00215E-4	0.18088	2.15183	3.19149E-5	2.52009E-12	0.00459
3.60015	8.753E-5	1.86875	4.33037E-4	0.1569	2.25892	3.16414E-5	3.4375E-12	0.00489
3.79998	1.11162E-4	1.52945	3.84339E-4	0.13977	2.34364	3.13845E-5	6.5245E-12	0.00424

Note: the abnormal parameters were labeled by red.

Table S9. Best fitted parameters obtained from the fits of the Cole-Cole plots of **1** under a zero dc field by employing a single relaxation Debye model.

T (K)	χ_S	χ_T	τ (s)	α	Residual
1.79993	0.69394	10.3555	0.01524	0.59455	0.20744
1.90009	0.822	9.35583	0.00888	0.55324	0.21842
1.99988	0.90878	8.62011	0.00569	0.51761	0.21645
2.10001	0.99431	7.96996	0.00387	0.48089	0.22209
2.20016	1.04546	7.49096	0.00283	0.45302	0.20771
2.29999	1.07714	7.07723	0.00212	0.42982	0.18089
2.40005	1.12553	6.70206	0.00165	0.40451	0.16928
2.50001	1.1547	6.39032	0.00131	0.38495	0.14555
2.60004	1.17071	6.09072	0.00105	0.36647	0.12855
2.79979	1.2096	5.5883	7.09566E-4	0.33543	0.08993
2.99986	1.25516	5.14509	5.05331E-4	0.30469	0.07129
3.20007	1.27291	4.76411	3.71288E-4	0.27984	0.05278
3.40008	1.27836	4.4418	2.82113E-4	0.26223	0.03813
3.60015	1.26345	4.14971	2.1714E-4	0.24754	0.03243
3.79998	1.20621	3.8924	1.6638E-4	0.23927	0.02557

Table S10. Best fitted parameters obtained from the fits of the Cole-Cole plots of **2** under a zero dc field by employing a single relaxation Debye model.

T (K)	χ_S	χ_T	τ (s)	α	Residual
1.81989	0.37678	0.69556	0.00473	0.55952	9.61126E-5
1.89994	0.36853	0.67615	0.00477	0.56131	3.95806E-5
2.00035	0.35864	0.6486	0.0042	0.55768	4.57287E-5
2.10006	0.34896	0.6203	0.00364	0.55226	4.62351E-5
2.2005	0.34087	0.59824	0.00329	0.54934	5.5583E-5
2.30164	0.33301	0.57626	0.00293	0.54512	6.28339E-5
2.40051	0.32588	0.55607	0.00265	0.54	7.29921E-5
2.59971	0.31436	0.51911	0.00226	0.52972	5.0508E-5
2.79999	0.30378	0.48648	0.00196	0.51604	5.00905E-5
3.00077	0.29351	0.45758	0.00173	0.50449	4.92126E-5
3.29985	0.28029	0.41984	0.00149	0.48405	3.98881E-5
3.69867	0.26469	0.37792	0.00131	0.452	3.61811E-5
4.09854	0.24829	0.34347	0.00114	0.43009	3.19318E-5
4.50162	0.23506	0.31454	0.00106	0.40284	2.20067E-5
4.99931	0.2188	0.28423	9.73097E-4	0.37506	1.39815E-5
5.50022	0.20396	0.25938	8.98321E-4	0.36091	1.01571E-5

Table S11. Best fitted parameters obtained from the fits of the Cole-Cole plots of **2** under a 1000 Oe dc field by employing a single relaxation Debye model.

T (K)	χ_S	χ_T	τ (s)	α	Residual
1.82003	0.36288	0.61035	0.00457	0.50803	8.81653E-5
1.99984	0.35492	0.58843	0.00492	0.50722	1.39485E-4
2.19993	0.33649	0.55963	0.00411	0.5154	1.66303E-4
2.40103	0.32228	0.531	0.00346	0.52186	9.06396E-5
2.60039	0.31134	0.50158	0.00292	0.51392	8.53909E-5
2.80036	0.29703	0.47542	0.00233	0.51713	9.60116E-5
2.99964	0.28591	0.44908	0.00187	0.51414	5.50132E-5
3.29902	0.27504	0.41646	0.0017	0.49855	6.39142E-5
3.59957	0.2636	0.38767	0.00155	0.49136	6.99034E-5
3.89838	0.25585	0.3574	0.00133	0.43636	3.05202E-5
4.20036	0.2439	0.33455	0.00118	0.43654	2.36718E-5
4.49894	0.23525	0.31655	0.00122	0.41817	4.12261E-5
4.79993	0.22525	0.29681	0.0011	0.40075	2.24541E-5
5.09741	0.21596	0.28062	0.00103	0.39309	1.43834E-5
5.39735	0.20752	0.26503	9.5265E-4	0.38056	8.53606E-6
5.69935	0.19912	0.25088	8.79362E-4	0.36583	7.26453E-6
5.99802	0.19263	0.23925	9.02599E-4	0.33528	9.93704E-6
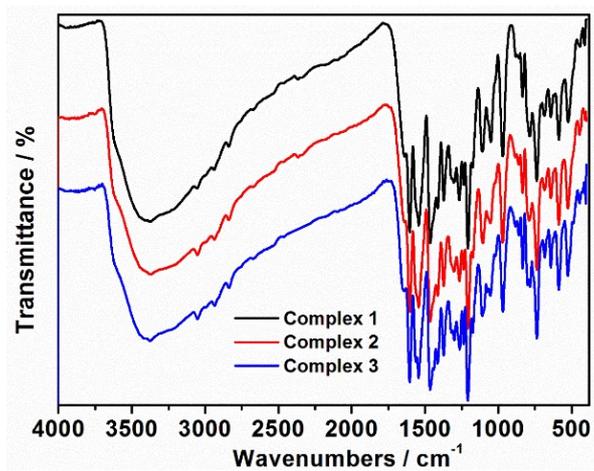
Figure S1. IR spectra of complexes **1-3**.
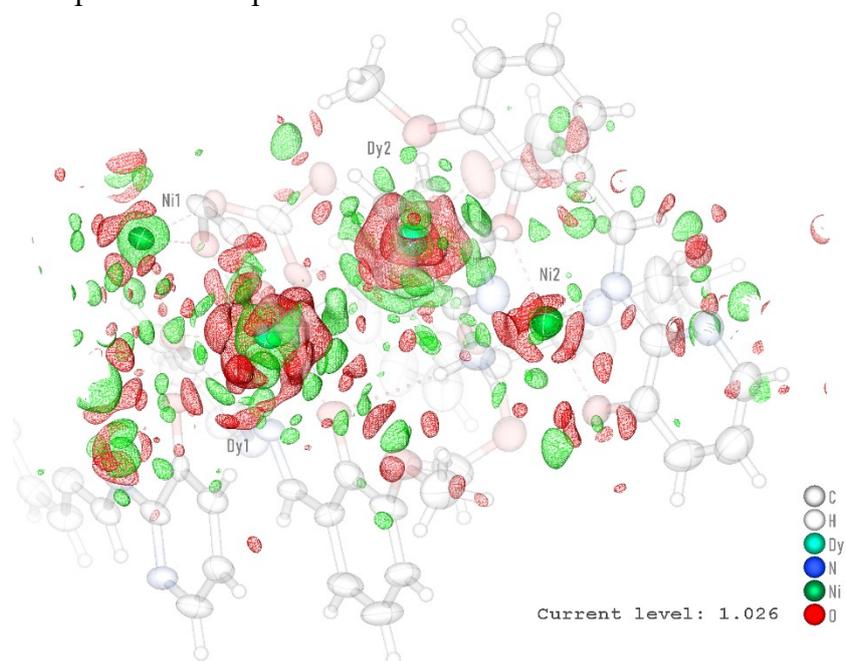
Figure S2. The large residuals around metal ions in **1**.
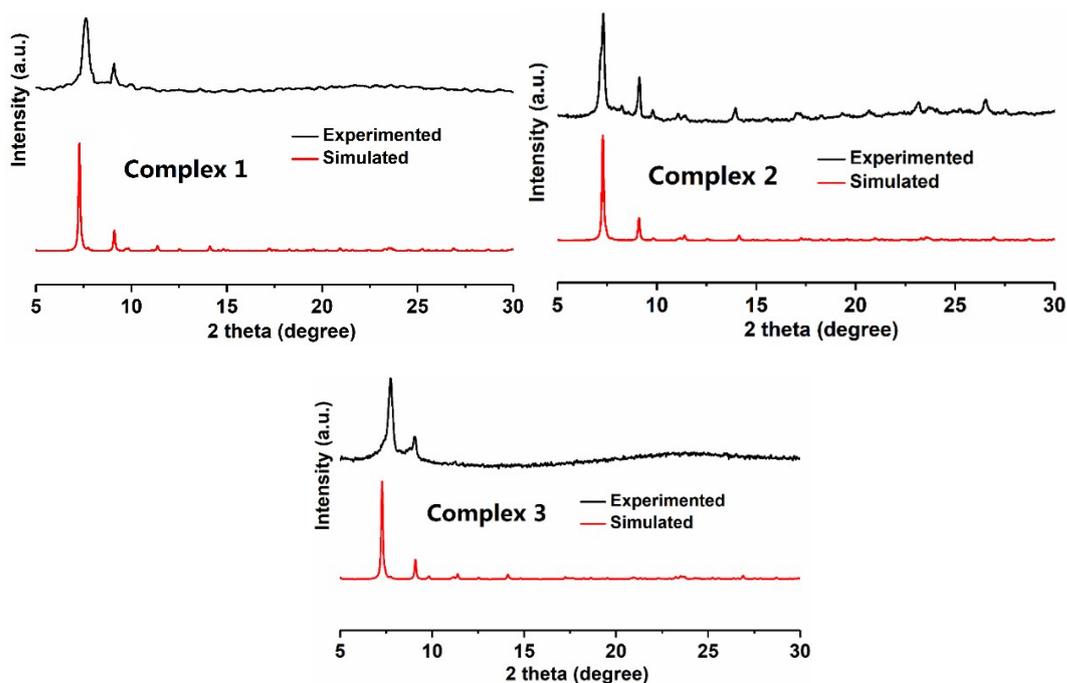
Figure S3. PXRD patterns and simulated patterns generated from single crystal diffraction data for complexes **1**-**3**.
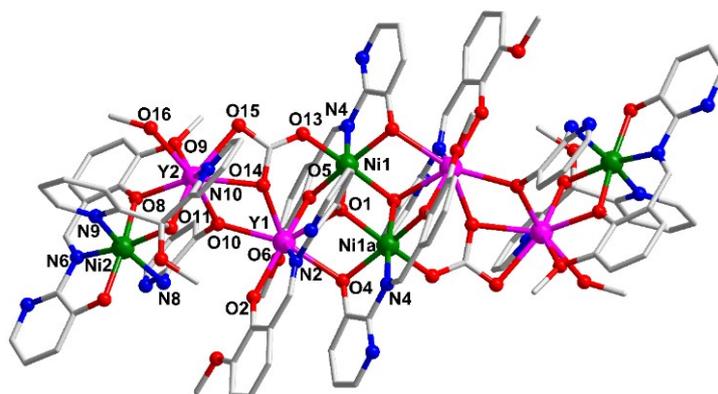
Figure S4. Crystal structure of **3**, in which Hydrogen atoms were omitted for clarity. Symmetry code: a = 0.5 − *x*, 0.5 − *y*, 1 − *z*.
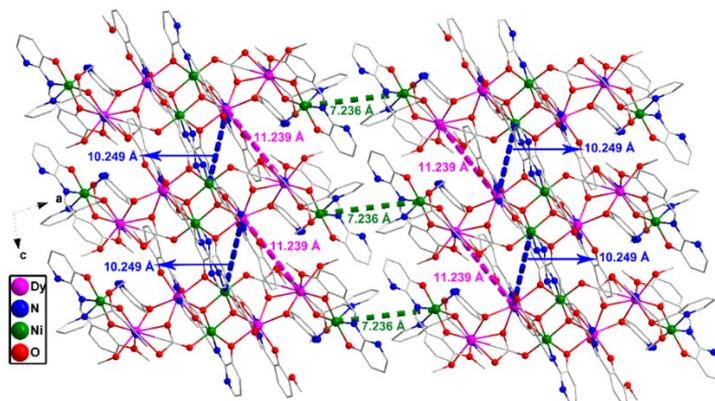

Figure S5. The plot viewing along *b* direction of crystal cell to show the distances of Dy^{III}···Dy^{III} (pink), Ni^{II}···Ni^{II} (green) and Dy^{III}···Ni^{II} (blue) in the neighboring molecules of **1**.
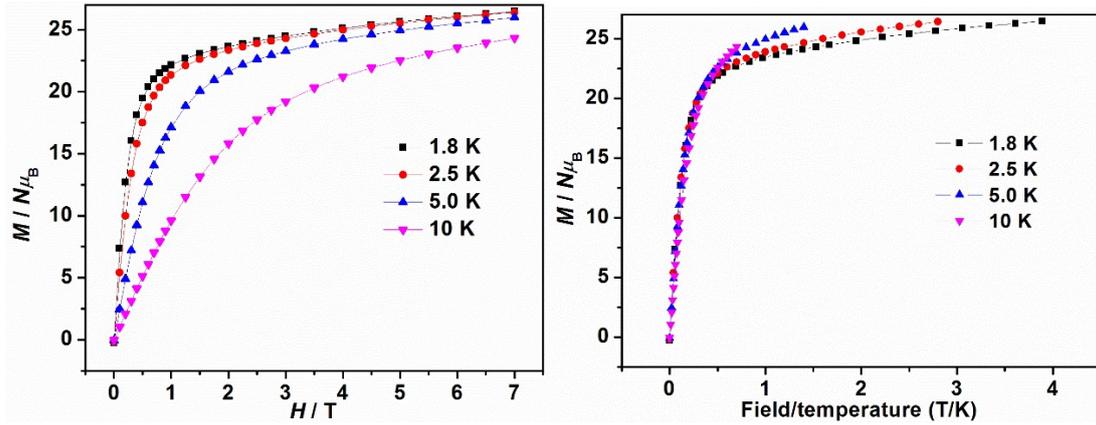
Figure S6. The plots of *M* *vs*. *H* (left) and *M* *vs*. *H/T* (right) for **1** measured in the range of 0-7 T and 1.8-10 K.
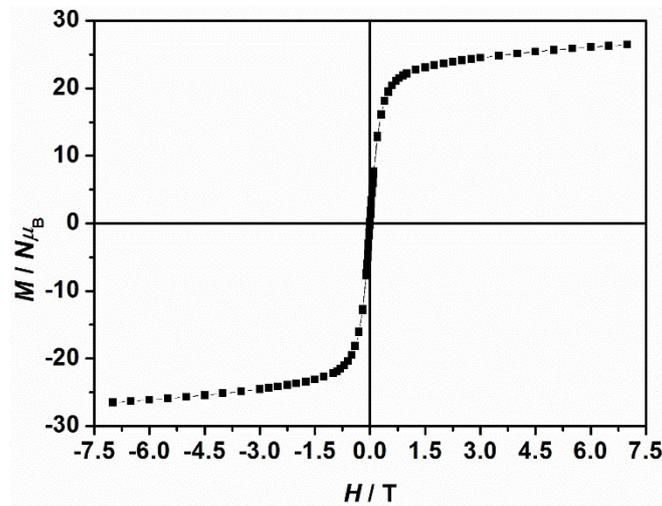
Figure S7. Hysteresis loops of **1** measured at 1.8 K (the field sweep rate is 0.02 T s^{-1}).
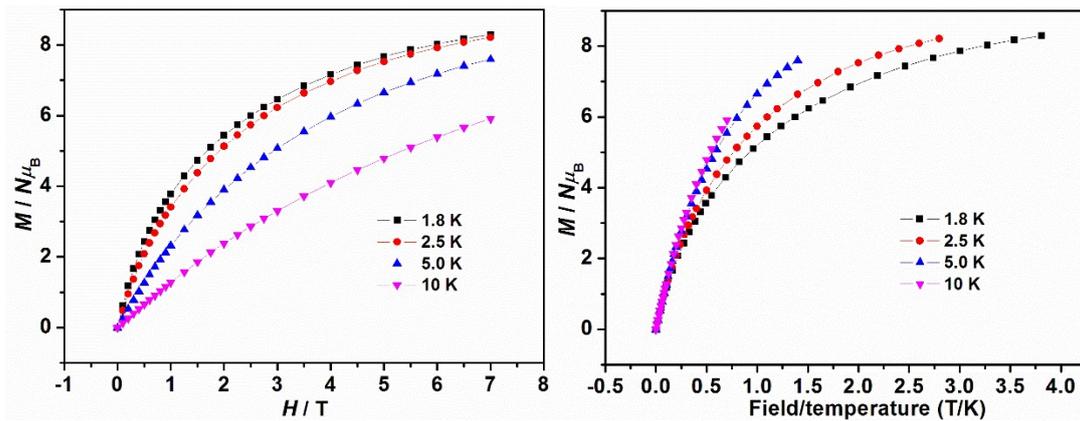
Figure S8. The plots of *M* *vs*. *H* (left) and *M* *vs*. *H/T* (right) for **2** measured in the range of 0-7 T and 1.8-10 K.
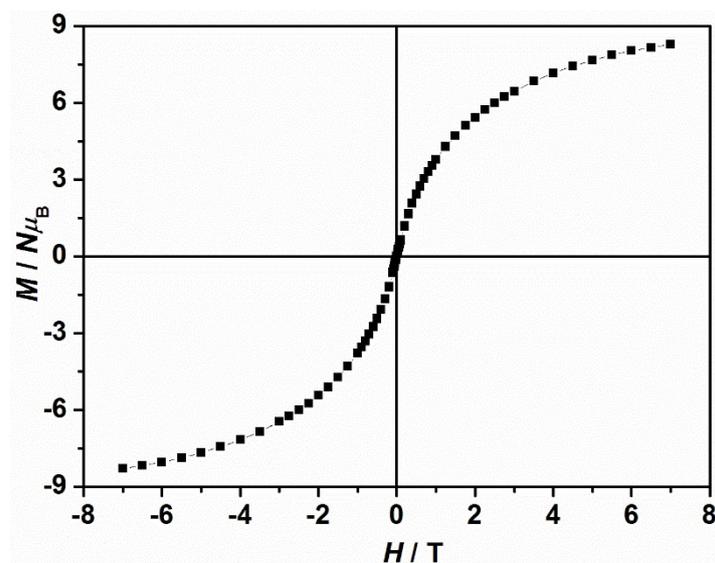
Figure S9. Hysteresis loops of **2** measured at 1.8 K (the field sweep rate is 0.02 T s^{-1}).
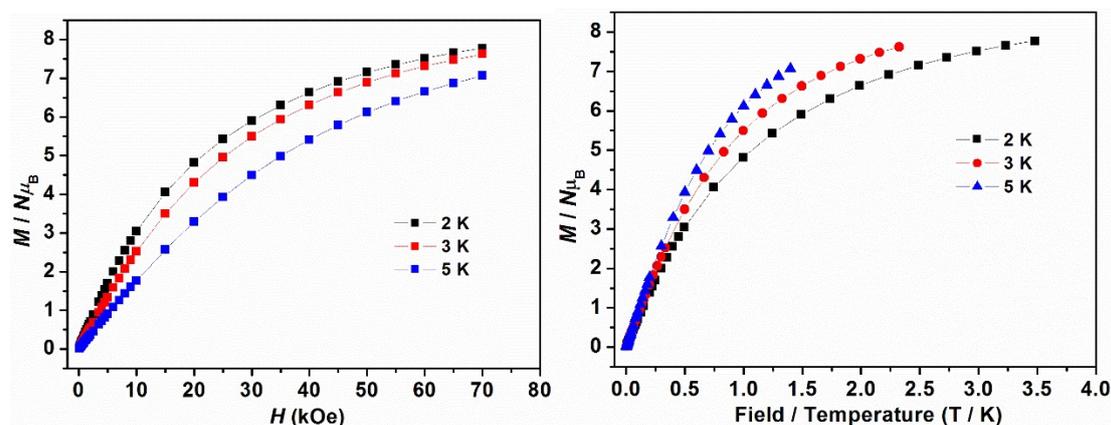
Figure S10. The plots of *M vs. H* (left) and *M vs. H/T* (right) for **3** measured in the range of 0-7 T and 1.8-10 K.
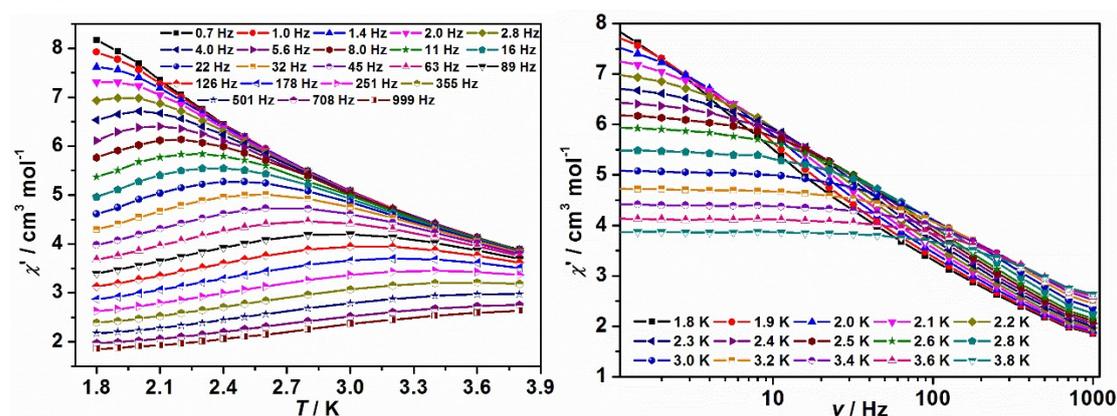
Figure S11. The plots of in-phase (χ') ac susceptibilities *vs. T* (left, *T* represents temperature) and χ' *vs. v* (right, *v* represents frequency) of **1** mesured under a zero dc field.
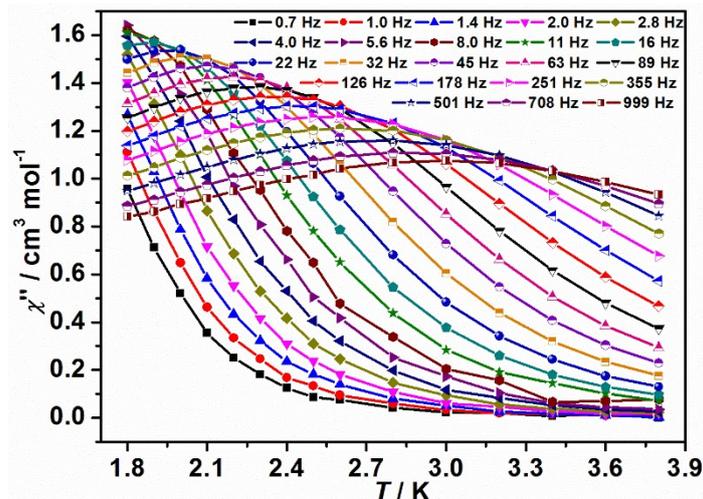
Figure S12. The temperature dependence of the out-of-phase (χ'') ac susceptibilities of **1** measured under a zero dc field.
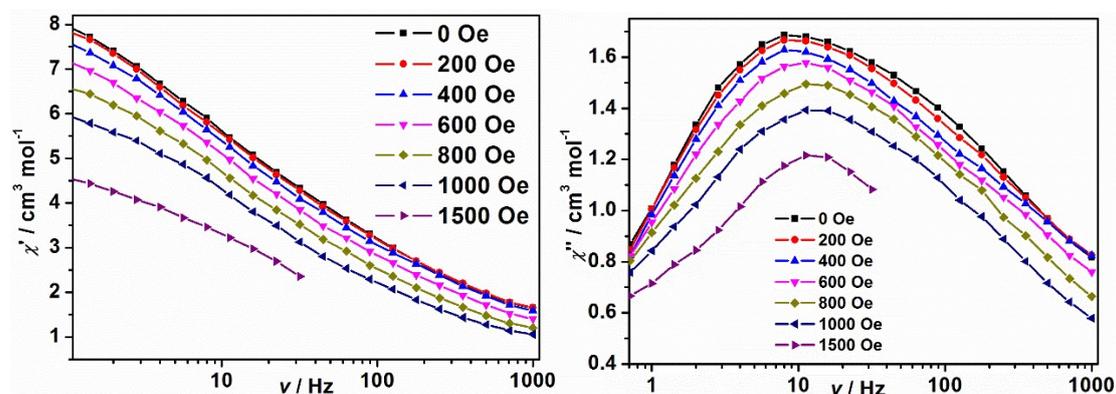
**Figure S13**. Frequency dependence of χ' (left) and χ'' (right) ac signals for **1** under different dc fields at 1.8 K.
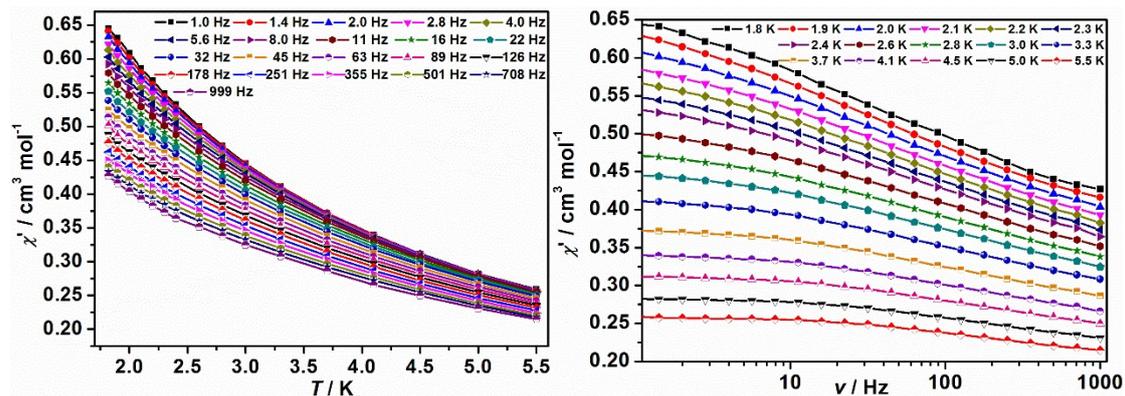

Figure S14. The plots of χ' *vs.* T (left) and χ' *vs.* v (right) of **2** mesured under a zero dc field.
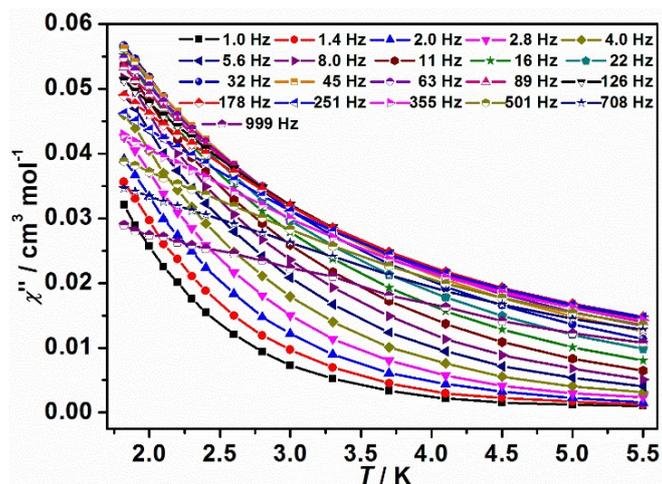
Figure S15. The temperature dependence of χ'' of **2** measured under a zero dc field.
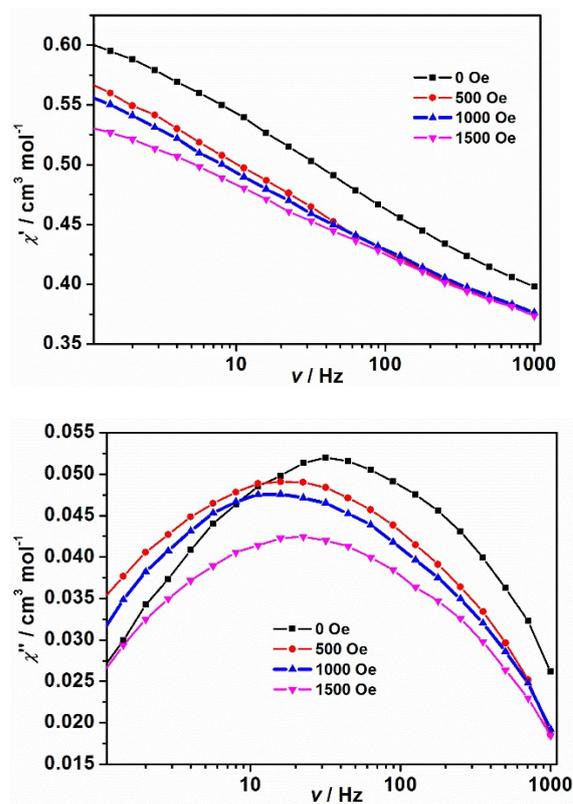
Figure S16. Frequency dependence of χ' (left) and χ'' (right) ac signals for **2** under different dc fields at 1.8 K.
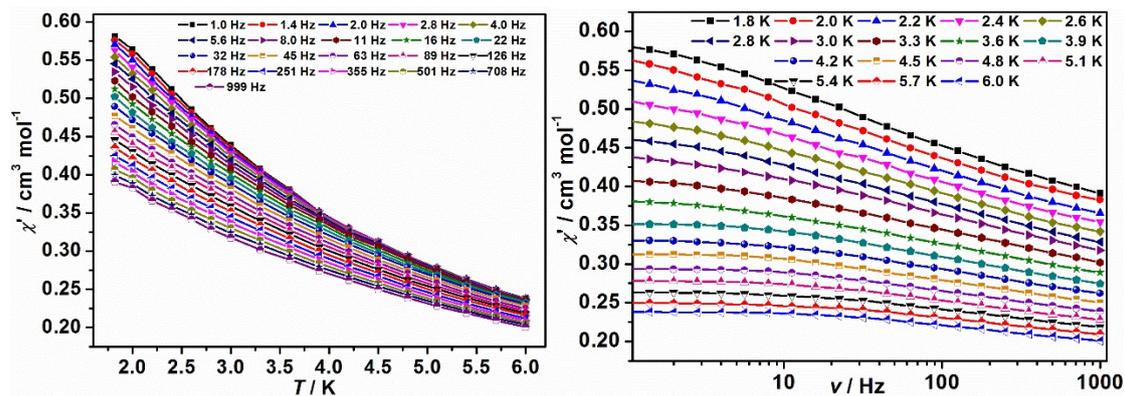
Figure S17. The plots of χ' *vs.* T (left) and χ' *vs.* ν (right) of **2** mesured under a 1000 Oe dc field.
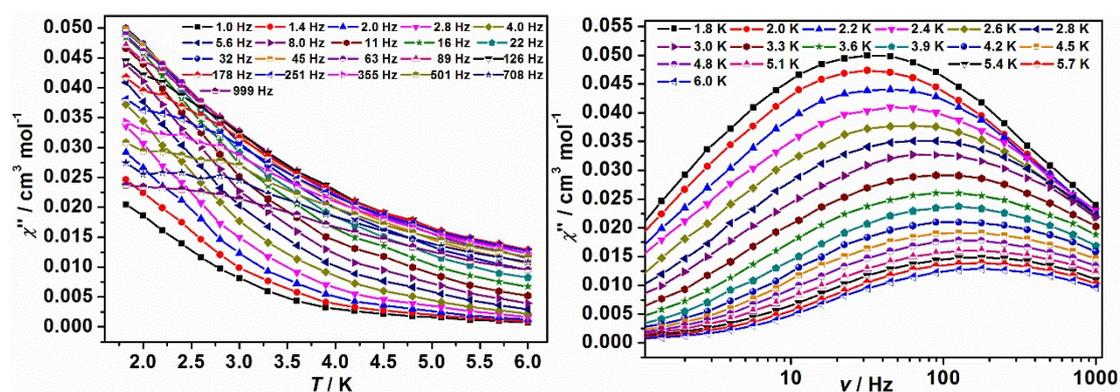
Figure S18. The plots of χ'' *vs.* T (left) and χ'' *vs.* ν (right) of **2** mesured under a 1000 Oe dc field.
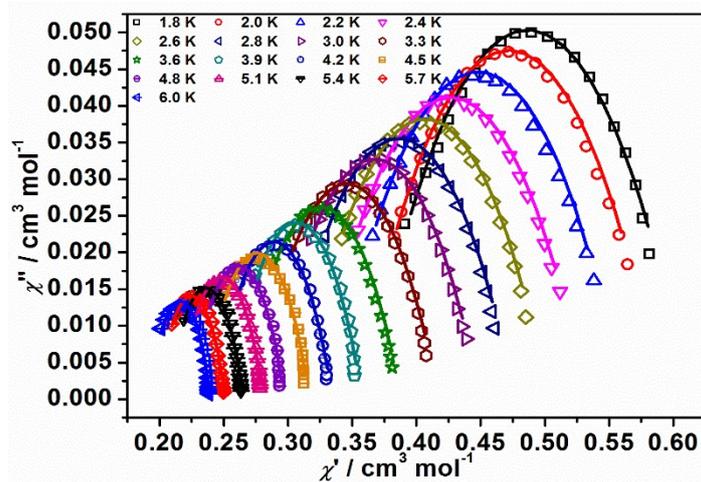

Figure S19. Cole-Cole plots of **2** under a 1000 Oe dc field, in which the solid lines represent the fitted results by the single relaxation Debye model.
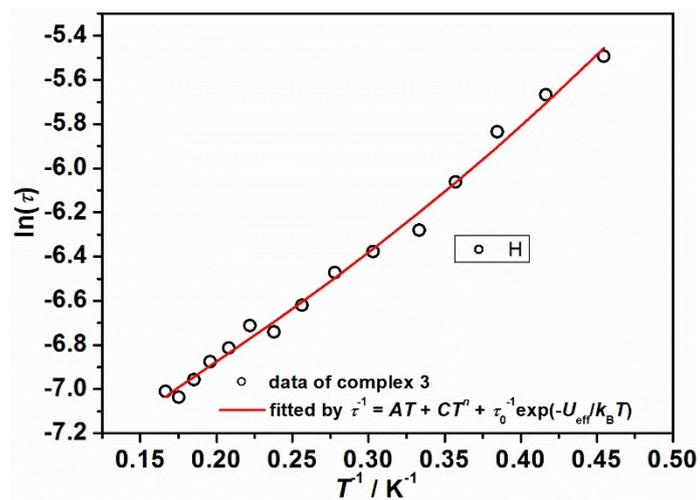
Figure S20. The plots of ln(τ) *vs.* T^{-1} of **2** under a 1000 Oe dc field; the red solid line represents the fit of relaxation data by employing the equation of $\tau^{-1} = AT + \tau_0^{-1}\exp(-U_{eff}/k_BT) + \tau_{QTM}^{-1}$.